

Residual Attention Guidance in Blindsight Monkeys Watching Complex Natural Scenes

Masatoshi Yoshida,^{1,2,6} Laurent Itti,^{3,4,6,*} David J. Berg,⁴ Takuro Ikeda,^{1,7} Rikako Kato,¹ Kana Takaura,^{1,2,8} Brian J. White,⁵ Douglas P. Munoz,⁵ and Tadashi Isa^{1,2}

¹Department of Developmental Physiology, National Institute for Physiological Sciences, Okazaki 444-8585, Japan

²School of Life Science, The Graduate University for Advanced Studies, Hayama 203-0193, Japan

³Computer Science Department

⁴Neuroscience Graduate Program

University of Southern California, Los Angeles, CA 90089, USA

⁵Centre for Neuroscience Studies, Queen's University, Kingston, ON K7L 3N6, Canada

Summary

Patients with damage to primary visual cortex (V1) demonstrate residual performance on laboratory visual tasks despite denial of conscious seeing (blindsight) [1]. After a period of recovery, which suggests a role for plasticity [2], visual sensitivity higher than chance is observed in humans and monkeys for simple luminance-defined stimuli, grating stimuli, moving gratings, and other stimuli [3–7]. Some residual cognitive processes including bottom-up attention and spatial memory have also been demonstrated [8–10]. To date, little is known about blindsight with natural stimuli and spontaneous visual behavior. In particular, is orienting attention toward salient stimuli during free viewing still possible? We used a computational saliency map model to analyze spontaneous eye movements of monkeys with blindsight from unilateral ablation of V1. Despite general deficits in gaze allocation, monkeys were significantly attracted to salient stimuli. The contribution of orientation features to saliency was nearly abolished, whereas contributions of motion, intensity, and color features were preserved. Control experiments employing laboratory stimuli confirmed the free-viewing finding that lesioned monkeys retained color sensitivity. Our results show that attention guidance over complex natural scenes is preserved in the absence of V1, thereby directly challenging theories and models that crucially depend on V1 to compute the low-level visual features that guide attention.

Results and Discussion

Efficiently guiding attention toward the most relevant parts of the visual world is a higher visual function critical for survival, as supported by many theories of attention [11, 12]. In most theories and computational models, V1 is the central site where visual features are computed that guide attention

toward salient locations [11–14]. Can blindsight patients or animals still compute such visual features? Although blindsight patients and animals exhibit significant residual visually guided behavior with simple laboratory tasks and stimuli, little is known quantitatively about their spontaneous natural vision (see [15, 16] for qualitative observations). Elucidating this question is important to understanding blindsight and the neural substrates of visual attention, and to possibly help affected patients better exploit residual visual processing in their daily life.

Macaque monkeys ($n = 6$) were trained to fixate and execute visually guided saccade tasks using simple stimuli. Primary visual cortex (V1) was then unilaterally removed in five monkeys by aspiration (as described previously [6]). Lesions covered at least 5° – 20° in eccentricity and $\pm 30^\circ$ around the horizontal direction for all monkeys (see Figure S1A available online). After the lesion, the presence of residual vision was confirmed with visually guided saccade tasks, reported previously [6]. Here we examined spontaneous eye movements of these monkeys during free viewing of 164 natural movie clips (~ 70 min). Successful central fixation for 0.5 s triggered a movie clip (4.0–93.8 s/clip), presented either normally or horizontally flipped to eliminate stimulus-induced biases. Monkeys did not receive juice reward during free viewing; thus, movies were not associated with reward. 128,361 saccades were recorded (Figure 1A).

First, we examined whether the basic properties of free-viewing saccadic eye movements were affected by V1 lesion. With both normal and horizontally flipped movies, distributions of fixations on the absolute screen area exhibited no strong left-right bias, for both intact and lesioned monkeys (Figure 1B). Moreover, there was no significant difference in data from normal versus flipped movies (Figure 1C), which were thus merged for saliency analysis below. Polar histograms of relative saccade vector directions (Figure S1B) showed no obvious left-right bias that might have been induced by lesion (Figure S1C). However, lesion did affect movie viewing. When polar histograms of saccade vectors were restricted to only the first saccade of each movie clip, they were significantly biased away from the affected field (Figures S1D and S1E). Note that such bias did not affect the overall distribution of saccade vectors because the first saccades comprise only 1% of all saccades (820 out of 75,767). Intact monkeys did not exhibit such bias (Figure S1E). We also detected effects of lesion on distributions of saccade amplitude and of peak velocity (Figures S1F and S1G). These results are consistent with our previous reports using laboratory stimuli, in that V1 lesion affects saccade dynamics [6, 8, 17].

Taking these results together, our analysis of free-viewing eye movements demonstrated surprisingly little effect of V1 lesion: lesioned monkeys still made many saccades to targets in their affected field and explored the stimulus screen area thoroughly. However, they also exhibited clear sensory deficits, as shown by the first-saccade bias toward the intact field, which is in agreement with previous studies using laboratory stimuli [4, 6].

To better understand how guidance of gaze was affected by V1 lesion in natural free viewing, we employed a computational

⁶These authors contributed equally to this work

⁷Present address: Center for Neuroscience Studies, Queen's University, Kingston, ON K7L 3N6, Canada

⁸Present address: Laboratory for Adaptive Intelligence, RIKEN Brain Science Institute, Wako 351-0198, Japan

*Correspondence: itti@usc.edu

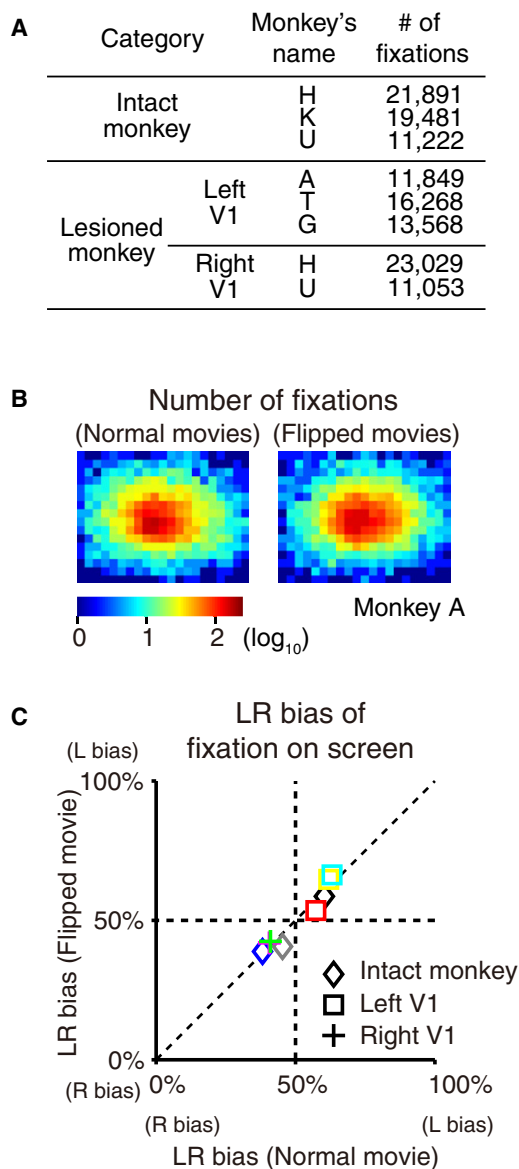


Figure 1. Basic Eye Movement Properties

(A) Number of saccades sampled in the free-viewing task for each of three monkey categories. In two monkeys (H and U), data were acquired both before and after lesion.

(B) Number of fixations on screen (monkey A) for normal (left) and horizontally flipped (right) presentations.

(C) Ratio of fixations on the left half of the screen to the total number of fixations (defined here as the LR bias) for normal movies (horizontal axis) versus horizontally flipped movies (vertical axis). Each symbol denotes data for a different monkey. The difference between the LR bias of normal movies and horizontally flipped movies was not significant ($p = 0.65$, paired t test, $n = 8$). See also [Figure S1](#).

model of visual saliency to quantitatively titrate the nature of visual targets that monkeys looked at. Briefly, the saliency model [18, 19] decomposed incoming video inputs along several simple visual features at multiple spatial scales. Center-surround contrast operators for six center and surround scale combinations gave rise to feature maps that highlighted locations that differed from their neighbors in each feature. Finally, all feature maps were combined into a single saliency map to emphasize conspicuous visual

locations in a feature-independent manner ([Figure 2A](#)). This model provides a flexible framework for predicting saliency maps from low-level feature maps, without necessarily committing to the exact origin or nature of the feature maps. Five features were used, each thought to contribute significantly to visual search in humans [20]: luminance, two chromatic contrasts (in the Derrington-Krauskopf-Lennie [DKL] color space derived from retinal ganglion cells [21]), orientation (V1-like Gabor filters in four orientations [22]), and motion (spatiotemporal energy model in four directions [23]). We quantified saliency-guided eye movements ([Figure 2B](#)) using receiver operating characteristic analysis of saliency values at endpoints of monkey saccades compared to random endpoints ([Figure 2C](#)) (see [Figure S2](#) for random endpoint sampling scheme). This resulted in an area under the curve (AUC) score (0.5 indicates chance performance, i.e., eye movements are not guided by saliency, whereas the best expected score, from interobserver correlation analysis, might reach ~ 0.7 ; see [Supplemental Experimental Procedures](#)).

AUC scores were significantly above chance for all monkeys ([Figure 2D](#)), indicating that lesioned monkeys were still significantly attracted toward salient targets in their affected field. At the population level, V1 lesions significantly reduced but did not abolish the tendency of monkeys to gaze toward salient targets (intact monkeys: $AUC = 0.627 \pm 0.002$; lesioned monkeys: $AUC = 0.601 \pm 0.003$ in affected field, $AUC = 0.627 \pm 0.003$ in normal field; see [Figure 2D](#) for statistical analysis). To investigate the possibility that some of the saccades into the affected field might be memory driven as opposed to truly visually guided, we duplicated the AUC analysis using only pure discovery saccades, i.e., saccades aimed toward screen locations that had never entered the intact field. The same pattern of results was observed ([Figure S2C](#)), excluding the possibility that memory was a dominant factor in directing saccades to the affected field.

Can we quantitatively explain differences in visual processing and saliency computations between normal and affected fields in term of features? To investigate this, we modified the model to examine relative contributions of the different basic features to gaze guidance. First, AUC scores were calculated for variants of the saliency model reduced to using only any one of our five features (“single-feature model”). All scores were significantly above chance, indicating that saliency in each feature taken separately still predicted monkey gaze above chance ([Figure 3A](#)). Because different features are often correlated in the natural visual world—e.g., a colorful object may also be brighter than the background, posing the question of whether color or brightness attracted attention ([Figure 3B](#))—we sought to isolate the nonredundant contribution of each feature to saliency. To this end, we used an optimization procedure followed by a leave-one-feature-out approach ([Supplemental Experimental Procedures](#)). The optimization algorithm adjusted the weights of the five features to maximize the model’s ability to predict monkey eye movements, separately for each of three different saccade groups (intact monkeys, affected field of lesioned monkeys, and normal field of lesioned monkeys, as defined in [Figure 2D](#)) ([Figure S3](#)). In the leave-one-feature-out approach, applied separately to each group, the AUC score of the optimized “full” model incorporating all features and the scores of each similarly optimized model incorporating all but one feature (“minus-one” model) were compared ([Figure 3C](#)). A nonredundant contribution index was defined as the AUC score difference between the full model and a reduced model divided

Residual Attention Guidance in Blindsight Monkeys

3

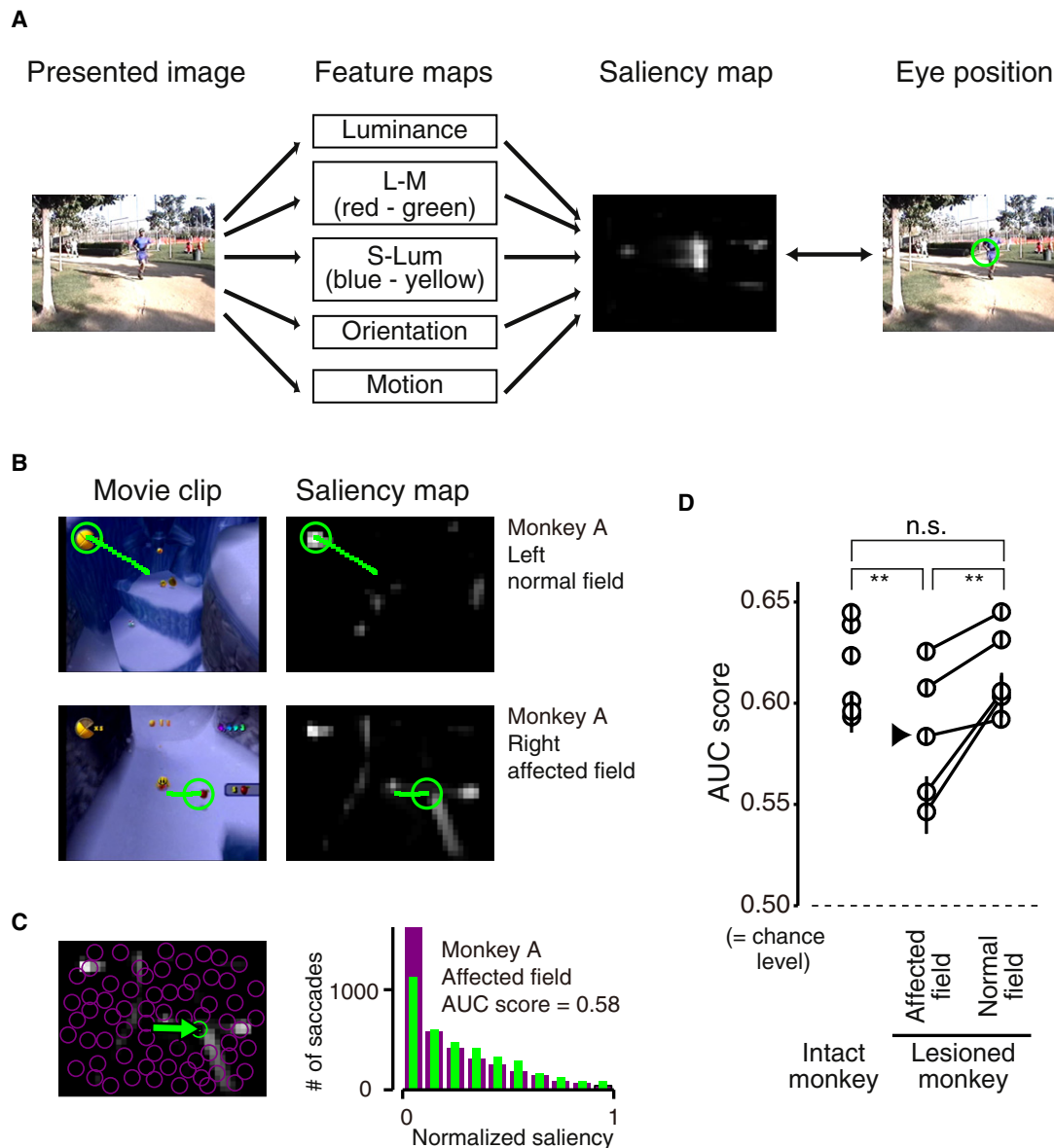


Figure 2. Residual Saliency-Guided Eye Movements after V1 Lesion

(A) Saliency model (see Supplemental Experimental Procedures for detailed definition of the features).

(B) Example movie frames (left) and saliency maps (right) with trajectory of an eye movement. Top: first saccade of a normally presented movie clip (movie 003, frame 5) directed leftward (normal field), toward a salient colorful object. Bottom: 91st saccade of the same clip (frame 1243) directed rightward (affected field), toward a salient moving object.

(C) Quantitative analysis of saliency-guided eye movements. Saliency values at each monkey saccade endpoint (green) and for random endpoints (magenta) were sampled (left) and histogrammed (right). Receiver operating characteristic analysis of the histograms yielded an area under the curve (AUC) score. AUC scores were computed separately for leftward and rightward saccades.

(D) AUC scores for three groups: “intact monkey,” data for left and right directions (six hemifields) for the three intact monkeys; “affected field” and “normal field,” data for the five lesioned monkeys. Error bars indicate SE. In all cases, AUC scores were significantly above chance (0.5) ($p < 0.05$, two-tailed t test). In group comparisons, ** indicates significant group mean difference ($p < 10^{-9}$, Wilcoxon signed-rank test after Bonferroni correction); n.s. indicates not significant ($p > 0.10$, Wilcoxon signed-rank test after Bonferroni correction).

See Figure S2 for consideration of sampling scheme.

by the AUC score of the full model minus 0.5 (Figure 3C). The index reflects how much a particular feature contributed to gaze guidance, beyond what could already be explained by the other four features. Figure 3D summarizes the contribution indices obtained. The pattern of feature contributions in intact monkeys resembled that in the normal field of lesioned monkeys (Spearman’s rank partial correlation $r = 0.90$, $p =$

0.09, $n = 5$), in which the contribution of motion is highest and those of color, orientation, and luminance follow (in decreasing order). After V1 lesion, however, that order shifted to motion, luminance, color, and orientation. This pattern did not resemble others ($r = 0.55$, $p > 0.2$ for affected field of lesioned monkeys versus intact monkeys; $r = -0.39$, $p > 0.2$ for affected field versus normal field of lesioned monkeys;

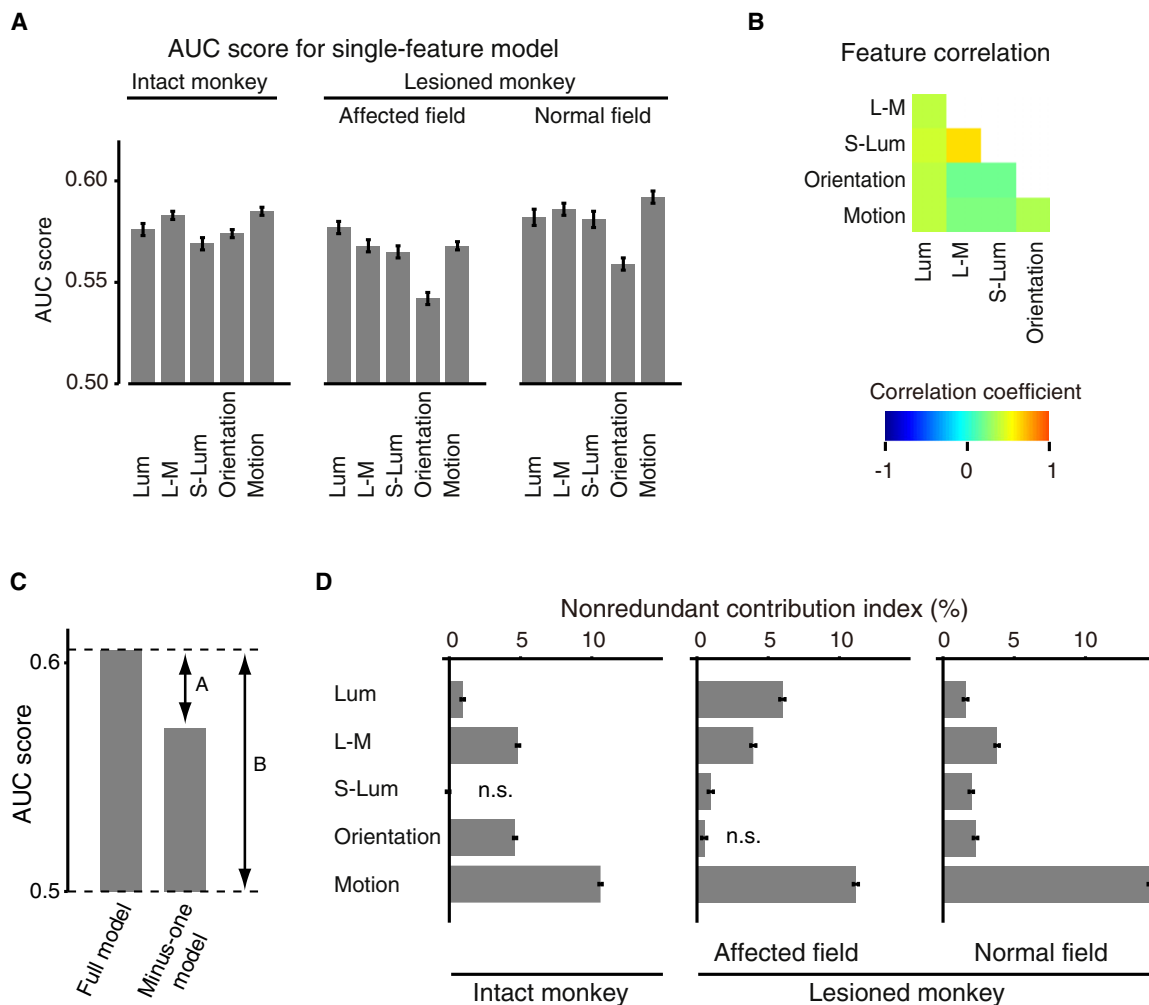


Figure 3. Contribution of Saliency for Each Feature

(A) AUC scores for single-feature models, for three groups as in Figure 2D, were all significantly above chance (0.5) ($p < 0.05$, two-tailed t test). Error bars indicate SE. Feature channels are as in Figure 2A. “Lum” denotes the luminance channel.

(B) Correlation coefficients between features over all movie frames used in the experiments were all significantly higher than zero ($p < 10^{-9}$ after Bonferroni correction).

(C) Variable-weight model. An optimized full model with all features was compared with a leave-one-feature-out model lacking one feature (“minus-one model”). The resulting differences between AUC scores (arrow A) were divided by the AUC score of the full model minus 0.5 (arrow B), which was used to define the nonredundant contribution index of the feature of interest (here, motion).

(D) Nonredundant contribution index of each feature (0 indicates that the feature of interest did not contribute to gaze guidance in any unique manner beyond what the other four features could predict). All of the feature contributions, except for those indicated n.s. (not significant), were significantly higher than zero ($p < 0.05$, paired t test, with Bonferroni correction for 15 simultaneous tests). Note that the contribution index does not add up to 100% (by definition). Error bars indicate SE.

Spearman’s rank partial correlation). Our analysis thus shows an interesting pattern of differences between intact and lesioned monkeys (Figure 3D): the contribution of orientation was decreased, luminance was increased, and motion and color remained relatively unchanged (see also the section “Consideration of Previous Results” in the Supplemental Information).

In Figure 3D, the finding that the contribution of color was not abolished in the affected field was surprising given contrasting results from previous laboratory experiments [3, 24–26]. This may be specific to our natural free-viewing paradigm. Hence, we designed a control laboratory experiment to verify the model’s prediction.

Two lesioned monkeys were tested with a visually guided saccade task using equiluminant chromatic stimuli (Figure 4A).

Lesioned monkeys detected, above chance, two types of equiluminant chromatic stimuli tuned to different ganglion cell types (Figure 4B). Although performance with chromatic stimuli was below that with high-contrast achromatic stimuli (positive control, confirming residual vision for luminance-defined shapes), it was better than for low-contrast achromatic stimuli (negative control, indicating that slight luminance differences between chromatic stimuli and background are unlikely to have contaminated chromatic processing). This was further confirmed in one monkey for a range of slight luminance variations (Figure 4C; see figure legend for detail). We further tested the monkey with color detection tasks using either mosaic stimuli or colored Gaussian stimuli to exclude possible contributions of edge artifacts and luminance differences (Figure S4). In sum, our

Residual Attention Guidance in Blindsight Monkeys

5

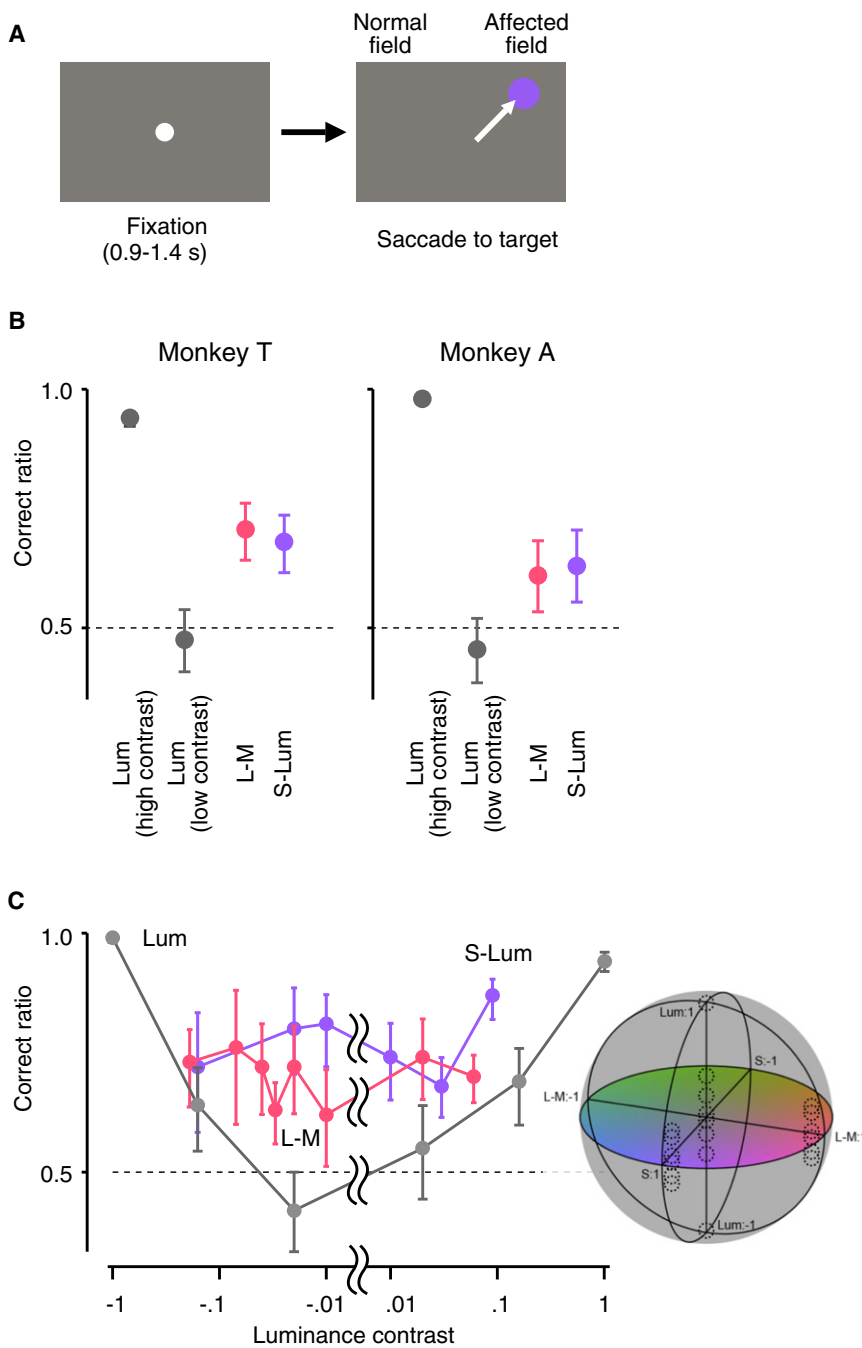


Figure 4. Direct Evaluation of Residual Chromatic Processing after V1 Lesion

(A) Visually guided saccade task using equiluminant chromatic stimuli. A single target stimulus was presented in the affected hemifield, either above or below the horizontal meridian. Correct forced-choice saccade to the target yielded fruit juice reward. Performance was evaluated by calculating the correct ratio as the number of trials with saccades toward the same quadrant as the target stimulus divided by the total number of trials with successful fixation before stimulus presentation.

(B) Performance for two lesioned monkeys (T and A). Lum (high contrast), achromatic stimuli with a luminance contrast of 2.3; Lum (low contrast), achromatic stimuli with a luminance contrast of 0.02 and -0.02 for monkey T and 0.04 and -0.04 for monkey A; L-M, equiluminant chromatic stimuli with isolated L-M channel stimulation; S-Lum, equiluminant chromatic stimuli with isolated S-Lum channel stimulation. Error bars denote 95% confidence interval. For Lum (high contrast), L-M, and S-Lum, but not for Lum (low contrast), performance was significantly above chance (0.5).

(C) Correct ratio for stimuli with small luminance difference added (horizontal axis) to account for possible contribution of deviations from exact equiluminance. Color coding is as in (B). Error bars denote 95% confidence interval. Data for monkey T are shown. Correct ratio remained significantly above chance for chromatic stimuli even over the range where it dropped to chance for luminance-defined stimuli, hence confirming that observed performance with chromatic stimuli was not due to contamination from luminance. Right: parameter of stimuli used in this experiment is depicted as dotted circles in the Derrington-Krauskopf-Lennie (DKL) color space.

control experiments using simple stimuli directly confirm residual guidance toward purely chromatic information, as predicted by our saliency model and free-viewing experiment. More broadly, color information was hence used during both forced-choice and spontaneous behavior in our blindsight animals.

In summary, for the first time, using a computational saliency model together with eye movement recording during free viewing of natural video stimuli, we observed sophisticated gaze orienting toward salient stimuli in blindsight. Our approach, combining computational modeling and free viewing, successfully allowed us to titrate the impact of V1 lesions on processing of visual features and the spontaneous

guidance of attention. Our results complement and extend previous laboratory experiments in a manner that is more relevant to daily life. It should be emphasized that our experiments and results concern detection and attention/gaze guidance, but not discrimination or identification. Thus, when we find that monkeys look toward stimuli in their affected field that are salient, e.g., in the color domain, this does not necessarily imply that the monkeys are capable of identifying or discriminating colors (see [Supplemental Information](#)).

Our study clearly shows that, after recovery, there is more to visual attention and saliency than the pathway through V1. We succeeded in pinpointing the features that guide residual vision, by expanding our original computational model to allow differential contributions of visual features. We believe that the use of natural movie stimuli is an important feature of the present study that places our results into a context more relevant to everyday life [27]. An important question for future research is whether the attention processes that we have shown to be active in postrecovery blindsight also contribute significantly to saliency, attention, and gaze even

in the normal brain. Our study also shows that computational models of attention cannot rely exclusively on V1 as the primary center for saliency computation [13], and that they should also consider how alternate pathways may provide critical feature information to the primate attention and saliency mechanisms.

Experimental Procedures

Six Japanese monkeys (*Macaca fuscata*; three male and three female, body weight 5–9 kg) were implanted with scleral search coils and a head holder (see [Supplemental Experimental Procedures](#)). All experimental procedures were performed in accordance with the National Institutes of Health Guidelines for the Care and Use of Laboratory Animals and were approved by the Committee for Animal Experiment at the National Institutes of Natural Sciences. After pretraining, V1 was surgically removed by aspiration under anesthesia in five monkeys. Free-viewing task was performed 15, 9, 28, 9, and 19 months after V1 lesion for monkeys A, H, T, U, and G, respectively. As a control, monkeys H and U were also tested before lesion, and intact monkey K was also tested. Monkeys watched 164 video clips that varied in duration and semantic content. Saccadic eye movements were determined using an algorithm that combined smoothed velocity measurements with a windowed principal components analysis [18]. A validated computational model of visual attention was used to predict individual eye movements ([Figure 2A](#)) [14, 19]. Two lesioned monkeys (T and A) were also tested with a visually guided saccade task with equiluminant color stimuli. Target stimuli were circular spots whose color properties were derived from the DKL color space [21].

Supplemental Information

Supplemental Information includes four figures and Supplemental Experimental Procedures and can be found with this article online at doi:10.1016/j.cub.2012.05.046.

Acknowledgments

This work was supported by the Human Frontier Science Program, the National Science Foundation, the Army Research Office, the Defense Advanced Research Projects Agency, Grants-in-Aid for Scientific Research (KAKENHI; 21500377 and 22220006), the Core Research for Evolutionary Science and Technology program of the Japan Science and Technology Agency, and the Excellent Young Researchers Overseas Visit Program of the Japan Society for the Promotion of Science. The views, opinions, and findings contained in this article are those of the authors and should not be interpreted as representing the official views or policies, either expressed or implied, of the Defense Advanced Research Projects Agency or the Department of Defense.

Received: March 18, 2012

Revised: May 1, 2012

Accepted: May 23, 2012

Published online: June 28, 2012

References

1. Weiskrantz, L. (1986). *Blindsight: A Case Study and Implications* (Oxford: Clarendon Press).
2. Payne, B.R., and Lomber, S.G. (2001). Reconstructing functional systems after lesions of cerebral cortex. *Nat. Rev. Neurosci.* 2, 911–919.
3. Cowey, A., and Stoerig, P. (2001). Detection and discrimination of chromatic targets in hemianopic macaque monkeys and humans. *Eur. J. Neurosci.* 14, 1320–1330.
4. Moore, T., Rodman, H.R., Repp, A.B., and Gross, C.G. (1995). Localization of visual stimuli after striate cortex damage in monkeys: parallels with human blindsight. *Proc. Natl. Acad. Sci. USA* 92, 8215–8218.
5. Weiskrantz, L., Barbur, J.L., and Sahaie, A. (1995). Parameters affecting conscious versus unconscious visual discrimination with damage to the visual cortex (V1). *Proc. Natl. Acad. Sci. USA* 92, 6122–6126.
6. Yoshida, M., Takaura, K., Kato, R., Ikeda, T., and Isa, T. (2008). Striate cortical lesions affect deliberate decision and control of saccade: implication for blindsight. *J. Neurosci.* 28, 10517–10530.
7. Kato, R., Takaura, K., Ikeda, T., Yoshida, M., and Isa, T. (2011). Contribution of the retino-tectal pathway to visually guided saccades after lesion of the primary visual cortex in monkeys. *Eur. J. Neurosci.* 33, 1952–1960.
8. Ikeda, T., Yoshida, M., and Isa, T. (2011). Lesion of primary visual cortex in monkey impairs the inhibitory but not the facilitatory cueing effect on saccade. *J. Cogn. Neurosci.* 23, 1160–1169.
9. Kentridge, R.W., Heywood, C.A., and Weiskrantz, L. (1999). Attention without awareness in blindsight. *Proc. Biol. Sci.* 266, 1805–1811.
10. Takaura, K., Yoshida, M., and Isa, T. (2011). Neural substrate of spatial memory in the superior colliculus after damage to the primary visual cortex. *J. Neurosci.* 31, 4233–4241.
11. Koch, C., and Ullman, S. (1985). Shifts in selective visual attention: towards the underlying neural circuitry. *Hum. Neurobiol.* 4, 219–227.
12. Treisman, A.M., and Gelade, G. (1980). A feature-integration theory of attention. *Cognit. Psychol.* 12, 97–136.
13. Li, Z. (2002). A saliency map in primary visual cortex. *Trends Cogn. Sci.* 6, 9–16.
14. Itti, L., Koch, C., and Niebur, E. (1998). A model of saliency-based visual attention for rapid scene analysis. *IEEE T. Pattern Anal.* 20, 1254–1259.
15. Humphrey, N.K. (1974). Vision in a monkey without striate cortex: a case study. *Perception* 3, 241–255.
16. de Gelder, B., Tamietto, M., van Boxtel, G., Goebel, R., Sahaie, A., van den Stock, J., Stienen, B.M., Weiskrantz, L., and Pegna, A. (2008). Intact navigation skills after bilateral loss of striate cortex. *Curr. Biol.* 18, R1128–R1129.
17. Isa, T., and Yoshida, M. (2009). Saccade control after V1 lesion revisited. *Curr. Opin. Neurobiol.* 19, 608–614.
18. Berg, D.J., Boehnke, S.E., Marino, R.A., Munoz, D.P., and Itti, L. (2009). Free viewing of dynamic stimuli by humans and monkeys. *J. Vis.* 9, 1–15.
19. Itti, L., and Koch, C. (2001). Computational modelling of visual attention. *Nat. Rev. Neurosci.* 2, 194–203.
20. Wolfe, J.M., and Horowitz, T.S. (2004). What attributes guide the deployment of visual attention and how do they do it? *Nat. Rev. Neurosci.* 5, 495–501.
21. Derrington, A.M., Krauskopf, J., and Lennie, P. (1984). Chromatic mechanisms in lateral geniculate nucleus of macaque. *J. Physiol.* 357, 241–265.
22. Daugman, J.G. (1980). Two-dimensional spectral analysis of cortical receptive field profiles. *Vision Res.* 20, 847–856.
23. Adelson, E.H., and Bergen, J.R. (1985). Spatiotemporal energy models for the perception of motion. *J. Opt. Soc. Am. A* 2, 284–299.
24. Brent, P.J., Kennard, C., and Ruddock, K.H. (1994). Residual colour vision in a human hemianope: spectral responses and colour discrimination. *Proc. Biol. Sci.* 256, 219–225.
25. Leh, S.E., Mullen, K.T., and Ptito, A. (2006). Absence of S-cone input in human blindsight following hemispherectomy. *Eur. J. Neurosci.* 24, 2954–2960.
26. Tamietto, M., Cauda, F., Corazzini, L.L., Savazzi, S., Marzi, C.A., Goebel, R., Weiskrantz, L., and de Gelder, B. (2010). Collicular vision guides nonconscious behavior. *J. Cogn. Neurosci.* 22, 888–902.
27. Nardo, D., Santangelo, V., and Macaluso, E. (2011). Stimulus-driven orienting of visuo-spatial attention in complex dynamic environments. *Neuron* 69, 1015–1028.

Current Biology, Volume 22

Supplemental Information

Residual Attention Guidance

in Blindsight Monkeys

Watching Complex Natural Scenes

Masatoshi Yoshida, Laurent Itti, David J. Berg, Takuro Ikeda, Rikako Kato, Kana Takaura, Brian J. White, Douglas P. Munoz, and Tadashi Isa

Supplemental Inventory

Figure S1 (related to Figure 1). This figure shows results of properties of vision and saccades, which has no space to display in Figure 1.

Figure S2 (related to Figure 2). This figure shows plots of the AUC values in different sampling schemes to demonstrate robustness of the finding in Figure 2D.

Figure S3 (related to Figure 3). This figure shows plots of weights of variable-weight model in Figure 3D to describe the summary of the procedure.

Figure S4 (related to Figure 4). This figure shows results of other color tasks to strengthen the conclusion drawn in Figure 4.

Supplemental Experimental Procedures

Supplemental References

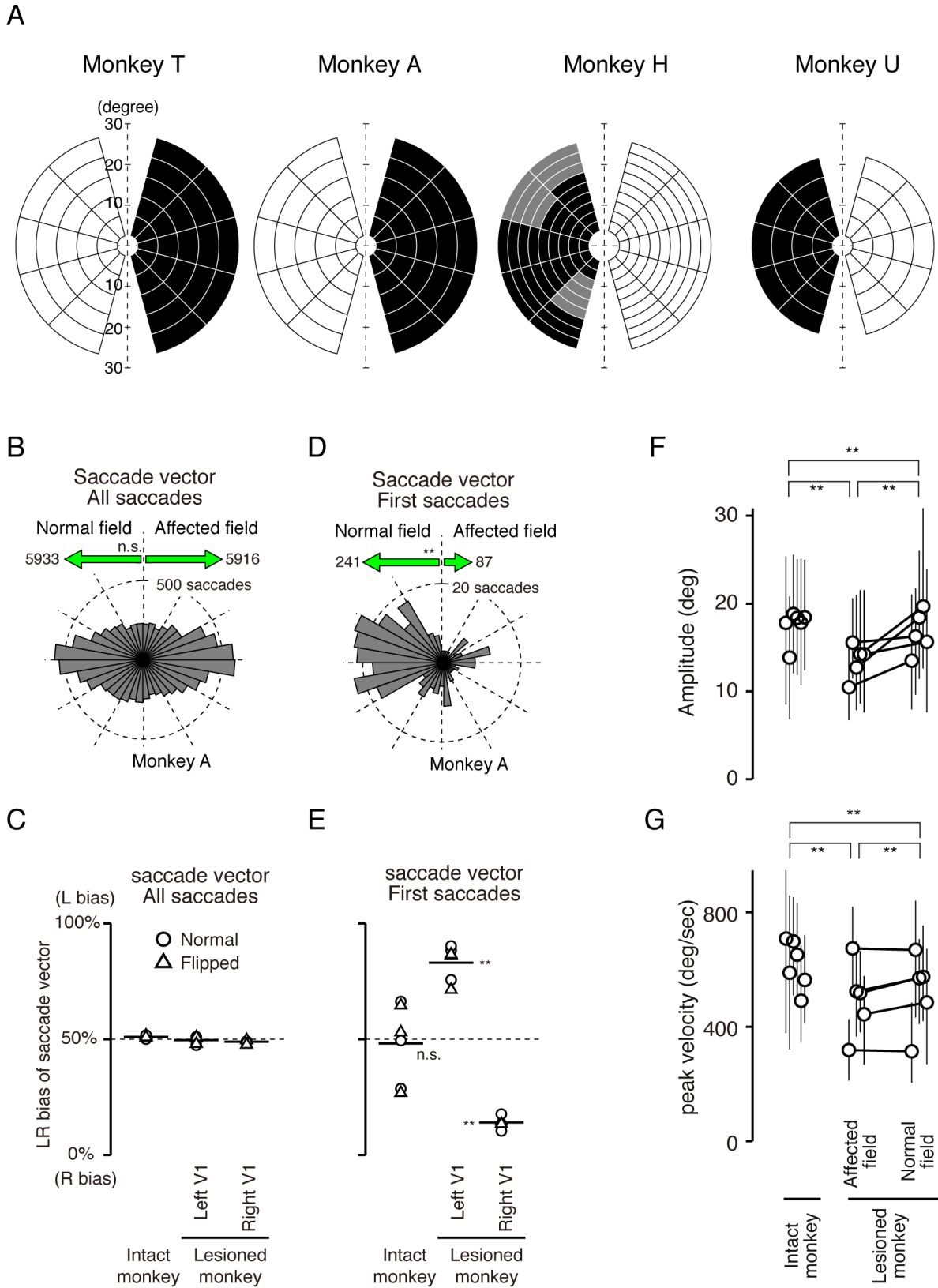


Figure S1.

Figure S1 (Related to Figure 1). Basic Property of Vision and Saccades

(A) Deficit maps. In four lesioned monkeys, visual sensitivity was tested with a visually guided saccade task. Black indicates the position where reduction of visual sensitivity was detected. Gray indicates the position where the sensitivity was not fully determined. White denotes control positions in their normal field. See Experimental Procedures for details.

(B and D) Polar histograms (monkey A) of the number of saccade vectors for all saccades (B) and the first saccades of each movie clip (D). The length of the green arrows is scaled to the total number of leftward or rightward saccades (numbers near the arrows). **, $p < 0.01$, binomial test. n.s., not significant.

(C and E) Ratio of the number of leftward saccades to the total number of saccades, plotted across three monkey categories (see Figure 1A). Each symbol denotes data for normal (circle) and horizontally flipped (triangle) movies of each monkey, for all saccades (C) and for the first saccades (E) of each movie clip. ** indicates significant deviation from 50% ($p < 0.01$, based on confidence interval calculated from maximum likelihood methods); n.s., not significant.

(F and G) Properties of saccades. The amplitude (F), the peak velocity (G) of saccades were plotted for three groups, in the same manner as in Figure 2D. The circles indicate the median value of saccades to each direction of each monkey. The error bar indicates 40% and 60% percentile of each population. **, significant difference between groups ($P < 10^{-9}$).

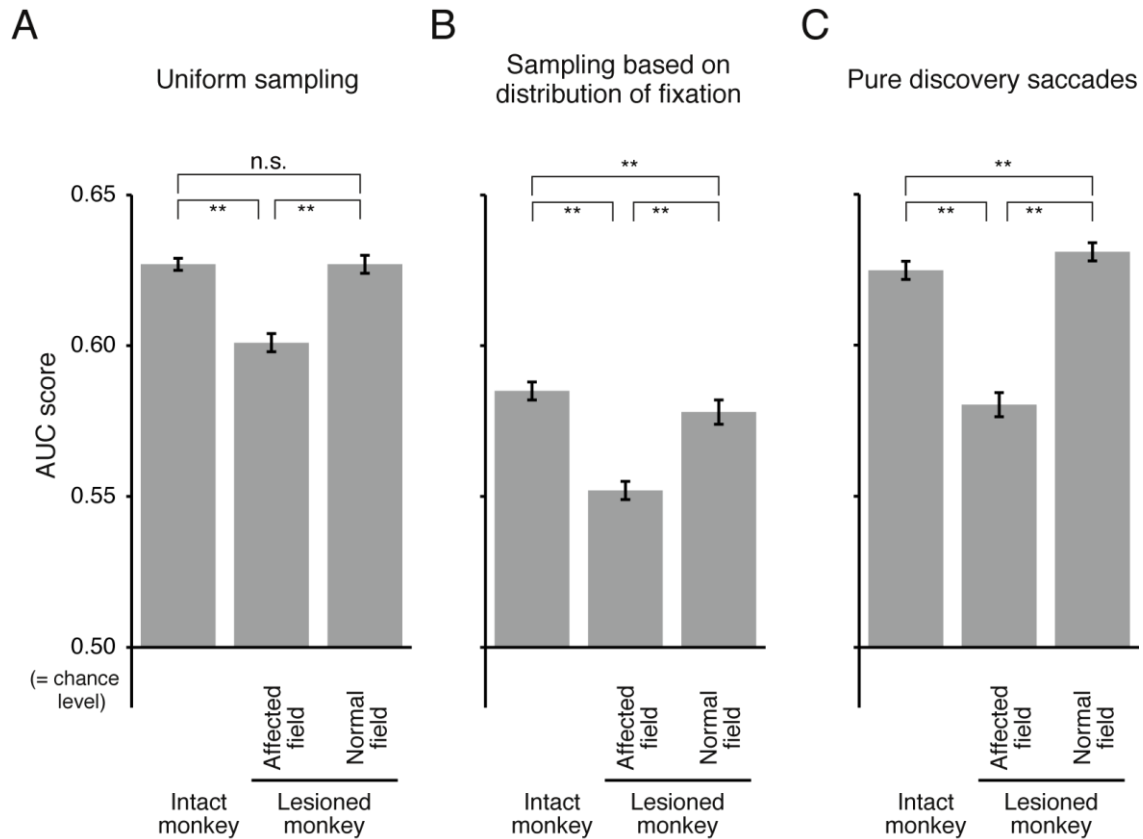


Figure S2 (Related to Figure 2). Consideration of Sampling Scheme

(A and B) AUC scores at the population level are plotted for three groups as in Figure 2D. For calculation of AUC scores, random sampling of saliency values was either (A) uniform or (B) drawn from the distribution of saccadic endpoints from all saccades made by the monkey group under test over the entire collection of video clips. The bar plot for (A) is identical to Figures 2D and displayed here for comparison. In the latter sampling scheme, the analysis of the AUC scores at the population level (B) gave essentially the same results as the original one (A); the AUC scores were significantly above chance for all three groups (intact monkeys: $AUC = 0.585 \pm 0.003$; lesioned monkeys: $AUC = 0.552 \pm 0.003$ in affected field, $AUC = 0.578 \pm 0.004$ in normal field).

(C) To exclude a possibility that the lesioned monkeys' saccades to the affected hemifield are guided by memory, another sampling scheme ('pure discovery saccades') was employed. We selected saccades which go into the affected field, and only counting those saccades which go to a screen location which has never before been inside the intact field. Note that this is a very strict test and should be interpreted as a lower bound of the AUC scores, rather than a quantification of saliency-guided eye movements, since those are only saccades to screen regions which have always been in the blind field. The AUC scores were significantly above chance for all three groups (intact monkeys: $AUC = 0.624 \pm 0.003$; lesioned monkeys: $AUC = 0.580 \pm 0.004$ in affected field, $AUC = 0.630 \pm 0.003$ in normal field). Error bars indicate S.E. In all cases, AUC scores were significantly above chance ($p < 0.05$, two-tailed t-test). In group comparisons, ** indicates significant group mean difference ($P < 10^{-9}$, Wilcoxon signed-rank test after Bonferroni correction); n.s., not significant ($P > 0.10$, Wilcoxon signed-rank test after Bonferroni correction).

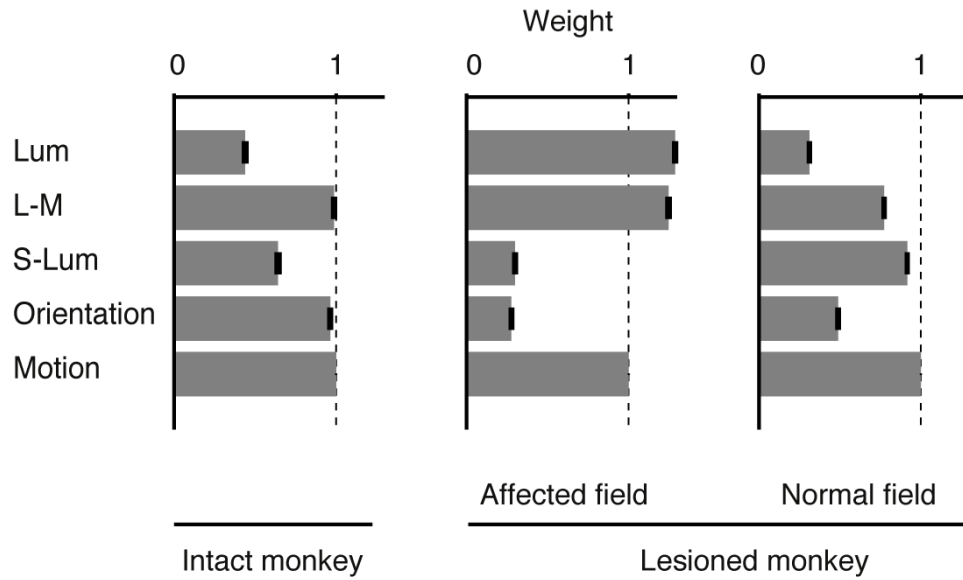


Figure S3 (Related to Figure 3). Weights for the Variable-Weight Models Incorporating All Features

Data is plotted for three groups as in Figure 2D. The weight for the Motion feature was set as one and other weights were expressed as relative values to that of the Motion feature. The error bars denote the standard errors calculated from the Hessians of the error surfaces (See Experimental Procedures). Note that the number of free parameters is not five but four since the AUC score depends on the relative value of weights, not the absolute one. The overall pattern of weights was similar to that of the contribution indices (Figure 3D), although weights do not take into account possible correlations across features, which are accounted for by the contribution indices.

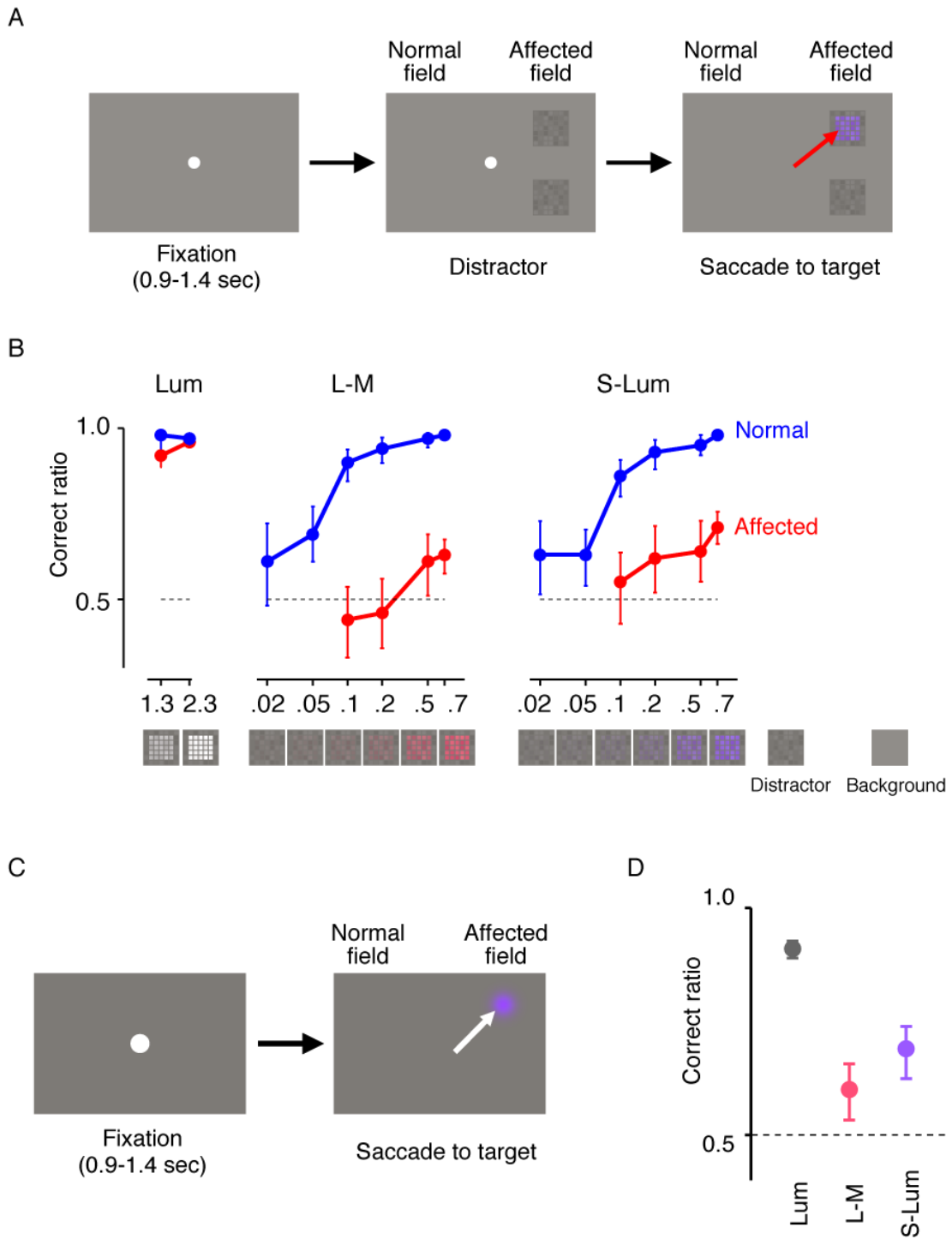


Figure S4.

Figure S4 (Related to Figure 4). Color Task Using Mosaic Stimuli (A and B) and Colored Gaussians (C and D)

(A) The task sequence. After fixation, identical distracters were presented both top and bottom of the affected field. After 0.5 sec, they were replaced by a target stimulus (top) with chromatic contrast and a distracter stimulus (bottom) without chromatic contrast. The monkeys were rewarded by making saccade to the target stimulus.

(B) The correct ratio was plotted for luminance contrasts of achromatic mosaic stimuli (Lum), for chromatic contrasts of mosaic stimuli (L-M and S-Lum). Red ('Affected'), the results of sessions where the stimuli were presented in the affected hemifield. Blue ('Normal'), the results of separate sessions where the stimuli were presented in the normal hemifield. Error bars indicate 95% confidence interval based on maximum likelihood method. In the bottom, examples of mosaic stimuli and distracters were shown.

(C) The task sequence is identical to the color task in Fig.4A. The only difference is that the stimuli are colored Gaussians with 10 degree SD.

(D. The correct ratio is plotted for luminance contrasts of achromatic mosaic stimuli (Lum), for chromatic contrasts of mosaic stimuli (L-M and S-Lum). Error bars indicate 95% confidence interval based on maximum likelihood method. Data are for monkey T.

Supplemental Experimental Procedures

Animal Preparation

Subjects

Six Japanese monkeys (*Macaca fuscata*; three male and three female, body weight 5-9 kg) were implanted with scleral search coils [1] and a head holder. All surgeries were performed under aseptic conditions as described previously [2]. Anesthesia was induced by administration of xylazine hydrochloride (2 mg / kg, i.m.) and ketamine hydrochloride (5 mg / kg, i.m.) and was maintained with isoflurane (1.0-1.5 %). All experimental procedures were performed in accordance with the National Institutes of Health Guidelines for the Care and Use of Laboratory Animals and approved by the Committee for Animal Experiment at National Institute of Natural Sciences. The monkeys were allowed to recover for more than 2 weeks before starting the prelesion training. The exact age of the monkeys is not known. Estimating from the body weight and the record of breeding history, all were operated at adult age except for monkey U that was operated at young adult age.

Prelesion Training

The monkeys sat in a primate chair with their heads in a fixed position and were trained to perform a fixation task and a visually guided saccade task for a liquid reward as described previously [2].

Unilateral V1 Lesion

To study residual vision after V1 lesion, it is important to exclude the possibility that spared cortex might contribute to residual vision [3, 4]. Thus lesion should cover all of the corresponding visual field tested (5-25 degrees in eccentricity). This corresponds to the posterior half of operculum, dorsal and ventral leaf and roof of calcarine sulcus and the most posterior part of the stem of calcarine sulcus [5-7]. Under anesthesia, these cortices were surgically removed by aspiration with a small-gauge metal suction tube. After surgery, the monkeys were given penicillin G (80 thousand units / day, i.m.) and cefmetazole (0.5 g / day, i.m.) as an antibiotics and dexamethasone sodium phosphate (0.5 mg / kg, i.m.) to minimize brain edema. Magnetic resonance images (MRIs) of the brains of these monkeys were acquired before and after the surgery to confirm anatomical lesion extent.

Postlesion Training

Postlesion training was started one to four weeks after V1 lesion, at which time the monkeys' general behavior in the cage appeared normal. Initial recovery after V1 lesion was assessed with the same task as during the preoperative training, as described previously [2]. Sensitivity for luminance contrast was assessed in all monkeys except for monkey G (who had not been trained for visually guided saccades tasks with stimuli with low luminance contrast), as described in [2]. The deficit map was drawn so that if the threshold for luminance contrast was significantly higher ($p < 0.05$, logistic regression) from the mirror-image position in normal hemifield, it was drawn as black (Figure S1A). For monkey H, threshold for some positions were not fully determined and the positions are displayed in gray (Figure S1A). The extent of lesion of monkey G was similar to that of monkey A or monkey U, and its deficit in free-viewing was also similar (Figure 2D and Figure S2B-C). We also tested whether some island of intact vision might have existed and might have been driving the main effect. We hypothesized that if such spared island of vision existed, salient stimuli presented at its eccentricity would more strongly attract saccades than salient stimuli at other eccentricities. Thus, we repeated our main analysis (Fig. 2D), but restricted it to different ranges of saccadic amplitudes ($<10^\circ$, $10..15^\circ$, $15..20^\circ$, $>20^\circ$). For each monkey, scores were remarkably similar across the different ranges of saccade amplitudes and always remained significantly above chance for all amplitude ranges ($p < 0.05$, t-test with Bonferroni correction; data not shown). In conclusion, our main effect (Fig. 2D) cannot be explained by a limited population of saccades towards a visual field location corresponding to a surviving island of cortex.

Free-Viewing Task

Stimulus Set

Monkeys watched 164 video clips (4.0 – 93.8 sec/clip, totaling approx. 70 minutes in duration, played in random order) that varied in duration and semantic content. The clips were composed of nature and/or complex movies. Stimuli were collected from television (NTSC source) with a commercial frame grabber (ATI Wonder Pro). The clip database included 15 so-called “monkey-relevant” clips collected at the Queen's University animal care facility with a consumer grade digital video camera [8], and depicting monkey facility environments, other monkeys, etc. Previous analysis of these clips compared to other natural clips revealed no significant difference, thus supporting that monkeys were engaged by all video clips in our collection [8]. Thus in the present study we used all 164 clips as a single video collection. Frames were acquired and stored at 30 Hz in raw 640 × 480 RGB555 format and compressed to MPEG-1 movies (640 × 480 pixels). Clips were presented either in their normal orientation or flipped horizontally, to eliminate possible stimulus biases towards left or right.

Task

The task was performed 15, 9, 28, 9, 19 months after V1 lesion for monkeys A, H, T, U, G, respectively. Visual stimuli were presented on a CRT monitor (21 inch, Mitsubishi RD21GZ, 71.5 × 53.5 cm; 640 × 480 pixels) positioned 28 cm from the eyes. This provided a usable field of view of 61.6° × 48.1°. Stimulus presentation was orchestrated using a Linux computer running in house-programmed presentation software (downloadable at <http://iLab.usc.edu/toolkit>) under SCHED_FIFO scheduling to ensure proper frame rate presentation [9, 10]. The task and data storage were controlled using computers running a real-time data acquisition system (Reflective computing, Tempo for Windows) with a dynamic link to Matlab (MathWorks). Trial initiation was self-paced. Each video presentation was preceded by a fixation point and the next video was initiated when the monkey's eye position remained within a square electronic window with 5° radius of the central fixation point for 500 ms. The monkeys were not rewarded for doing this task, but the monkeys quickly learned to fixate in order to initiate the next clip. (In calibration sessions, they were rewarded by fruit juice for correctly making saccades and fixations to simple objects.) After each clip, a 1.5 sec inter-trial interval followed, and the next trial began as the fixation spot turned on.

Eye-Tracking and Calibration for Saccade Measurement

Monkeys were seated in a primate chair with their heads restrained. Eye movements were recorded using a magnetic search coil [11] with a resolution of 0.1 degree. Horizontal and vertical eye positions were sampled at 1 kHz. To calibrate eye position, monkeys performed a fixation task in which targets at nine different horizontal positions and at nine different vertical positions were presented. Monkeys were given a liquid reward if they fixated a target within a circular window for 1 sec. The window was variable across eccentricities from the fixation point at the center of the screen, typically, 4 degrees radius at 10 degrees eccentricity and 7.5 degrees radius at 20 degrees eccentricity. The mean eye position during 750-1000 ms of the fixation period was used for calibration. In order to control for small non-linearities in the field coil, the weighted average of several visits to each target endpoint was later used to perform an affine transform and thin-plate-spline interpolation [10] on the eye position data collected during free viewing of the video clips. This calibration session was performed both before and after the free-viewing sessions.

Quantifying Eye Movement Behavior

Saccadic eye movements were determined using an algorithm which combined smoothed velocity measurements with a windowed principal components analysis (see [8] for details). For analysis with the saliency model, saccades with short (<80 ms) intervening fixations or smooth pursuits and small differences in saccadic direction (<45°) were assumed to represent readjustments of gaze en route to a target, and so were combined into a single saccadic eye movement toward the final target, rather than two or more separate saccades. Additionally, saccades of <2° in amplitude and <20 ms in duration were removed in order to decrease the false positive rate of saccade parsing and to focus analysis on eye movements that more likely reflected a shift of attention to a new target as opposed to minor gaze adjustments on a current target [10]. This saccade parsing algorithm is freely available as part of the open-source stimulus presentation software.

For the model-free analysis of Figure 1, all 128,361 fixations recorded were used, as detailed in Figure 1A, under the assumption that whether or not the monkey paid attention to the stimuli was irrelevant

to basic saccade statistics. For analysis with the saliency model, however, we first eliminated clips and fixations where monkeys were presumably not engaged by the video stimuli, as detailed below. For each monkey, clips that contained too few eye movements (fewer than 10 saccades per clip) or excessive off-screen eye movements, suggestive of sleeping or inattentive behavior (more than 10% of saccades ending off-screen, or more than 70% of viewing time spent off-screen) were excluded from the analysis. This procedure reduced the total fixation pool from 128,361 to 99,170. We also removed saccades shorter than 4° or longer than 25° to focus the analysis onto the part of the visual field which was affected in all lesioned monkeys. In total, 73,453 fixations were used for the analysis that used the saliency model.

Computational Modeling

Implementation

To assess the visually guided behavior of monkeys, a validated computational model of visual attention were used to predict individual eye movements (Figure 2A). Models were created and run under Linux using the iLab C++ Neuromorphic Vision Toolkit [12]. We used the saliency model of visual attention framework (Figure 2A) [13, 14]. The Itti and Koch model computes salient locations by filtering the movie frames along several feature dimensions (color, intensity, orientation, and motion). Center-surround operations in each feature channel highlight locations that are different from their surroundings. Finally, the channels are normalized and linearly combined to produce a saliency map, which highlights screen locations likely to attract the attention of human or monkey observers. To account for a wide range of spatial frequencies of oriented stimuli, our model uses 9 spatial scales of Gabor filters, with the following spatial frequencies in cycles/degree (given the screen size, resolution, and viewing distance): 1.1500, 0.5750, 0.2875, 0.1437, 0.0719, 0.0359, 0.0180, 0.0090, 0.0045. This range includes relatively lower spatial frequency, for which blindsight has been shown to be sensitive when detecting orientation gratings (e.g., [15]).

Comparing Eye Movements to Model Output

To compute the performance of each model, the map values in a window ($1.75^\circ = 16$ pixels) around saccadic endpoints were compared to 1200 map values collected from locations randomly chosen. Random sampling was either uniform or drawn from the distribution of saccadic endpoints from all saccades made by the monkey under test over the entire collection of video clips. This approach is similar to the image-shuffled analysis method used by others for static images [16-18] and allows evaluation of model performance while discounting possible effects of center bias. For a particular subject, at the onset of a saccade we measured the value in each model map at the endpoint of the saccade, i.e., the activity in the map just before the saccade.

Saliency values at monkey vs. random saccade endpoints were analyzed through ROC analysis, giving rise to an AUC score as described in the main text. An AUC score of 0.5 indicates that the saliency map model under study is not able to predict monkey eye movements better than chance. Although in theory the maximum achievable score is 1.0, in practice this cannot be reached because of natural variability of eye movements across observers: It is not possible to build a single computational model which can exactly pinpoint the single location of every monkey saccade, since different animals often do not look at the same location. In previous studies using the same AUC scoring technique, we have shown that a practical upper bound on achievable AUC scores given inherent inter-observer variations is around 0.7 [8, 19, 20].

Model Optimization Procedure

To evaluate the unique, non-redundant contributions of different visual features to eye movements, we employed an optimization procedure (Figure 3). We compared the AUC score of the best-fitting model that includes all features to that of the best-fitting model that includes all but one features. Optimization was carried out using a Simplex algorithm [21] which was run several times from randomly chosen starting points to ensure convergence to the global optimum. The optimization procedure gave rise to an optimum set of feature weights that maximized AUC for each variant of the model and each monkey population under consideration. To assign error bars to the best-fitting weights, we computed the local Hessian of the AUC score with respect to the feature weights, and used this to convert a tolerance of ± 0.01 on the AUC value into the corresponding tolerance onto weight values. The procedure is as described in [22]. This

method allows us to gauge how tightly constrained a given weight is by the eye movement data, as reflected by the final error bars on weight values.

Evaluation of Color Sensitivity

Visually Guided Saccade Task with Equiluminant Chromatic Stimuli

At the beginning of each trial, the fixation point (FP) appeared at the center of the screen, and monkeys were required to move their eyes to the FP. The duration of fixation was varied randomly between 400 and 1000 ms. If the eye position deviated more than 1.5 degrees from the FP, the trial was aborted. The saccadic target appeared in the peripheral visual field concurrently with the offset of the FP. Monkeys were rewarded with fruit juice 200-500 ms after correctly making a saccade to the target and then maintaining fixation for 100-300 ms in the target window (size 2-3 degrees). Target eccentricity was fixed at 10 degrees. Target direction was either upper 30 degrees or lower 30 degrees for both hemifields. A small percentage of trials with saccadic reaction times less than 80 ms were considered to be trials with anticipatory saccades and were omitted from the analysis. Trials with saccadic reaction times greater than 700 ms were rare and were also omitted from the analysis. Inter-trial intervals ranged from 1500 to 2000 ms.

Visual Stimuli

Target stimuli were circular spots whose color properties were derived from the Derrington–Krauskopf–Lennie (DKL) color space [23, 24]. This color space corresponds closely to the type of segregation that exists along the geniculostriate pathway in early vision [24]. One pathway sums the inputs of the long- and middle-wavelength cones (L + M), producing a luminance channel that is mostly sensitive to stimuli varying along the “black–white” dimension in the DKL space. A second pathway computes the difference between the inputs of the L and M cones (L - M), and is mostly sensitive to stimuli varying along the “red–green” dimension in the DKL space. A third pathway computes the difference between the inputs of the short-wavelength cones (S-cones) with the sum of the L- and M-cones [S - (L + M)], and is mostly sensitive to stimuli varying along the “blue–yellow” dimension in the DKL space. These three channels form the primary visual-cortical inputs via the magnocellular, parvocellular, and koniocellular layers of the LGN, respectively.

The monitor phosphors were measured using a photo-spectrometer (PR-650, Photoresearch, CA, USA), and the resulting CIE xyY values were used to convert between RGB and DKL color space by the Stockman & Sharpe cone fundamental [25]. The Stockman & Sharpe cone fundamental are based on human data there is a good match with macaque cone sensitivities (e.g. [26]), although there is a caveat that relative numbers of cone types may differ [27]. The target color stimuli were presented against an isoluminant (25 cd/m²) neutral gray background. The luminance contrast was expressed as Weber contrast, thus the luminance contrast of the black stimuli was represented as -100%. For chromatic stimuli, the saturation was expressed as the percentage of maximum achievable stimuli by the CRT monitor for L-M and S-Lum axis.

The size of the target was 0.45 and 0.90 degrees in diameter for monkey T and A, respectively. Luminance of the background and the target was set to 25 cd/m². The size of the target for monkey T was set so that the monkey cannot respond to the equal size of achromatic target with high luminance contrast (0.9 in Michelson contrast) and with dim background luminance (1 cd/m²) presented in the blind spot, thus ensuring no contribution of light scattering to residual vision. The size of the target for monkey A was set so that the performance of achromatic stimuli was comparable to that of monkey T.

For a control experiment in Figure 4C, we varied luminance of the chromatic stimuli. The range of luminance added to the chromatic stimuli was from -16% to +16%, which is maximal in the DKL space when the saturation of the stimuli is 90% of the maximally attainable value in our monitor.

Analysis of Performance

Performance was evaluated by calculating the correct ratio, as the number of trials with saccades toward the same quadrant as the target stimulus divided by the total number of trials with successful fixation before stimulus presentation. Saccades were detected when the peak velocity of the polar component exceeded 200 degrees/s. Then the onset time of the detected saccade was defined as the time point preceding the detected saccade at which the velocity exceeded 30 degrees/s. The end point of the

saccades was defined as the spatial position at which the velocity of the saccade declined below 30 degrees/s after the saccadic onset. For statistical analysis, Matlab (MathWorks) was used.

Color Task Using Mosaic Stimuli

The mosaic stimuli are composed of 7 by 7 patches. For distractor (Figure S4), the luminance contrasts of 49 patches were sampled from uniform distribution with the mean luminance 25 cd/m², identical to the background luminance, and with a range from 80% to 120% of Weber contrast (20-30 cd/m²). In each trial, the same 49 patches were chosen but the positions were shuffled. The two distractors presented before fixation offset were identical. For target, the only difference from distractor was that a constant chromatic contrast (either L-M or S-Lum) was added to the central 5 by 5 patches. After the fixation point was extinguished, both the target and the distractor were presented. Both of them had the identical mosaic pattern and the pattern was different from the pretarget distractors. Therefore, the subject could not use either the pattern of mosaic nor change detection but chromatic contrast to detect the target stimuli. Chromatic contrast was calculated as the ratio of L-M or S-Lum value to the maximally attainable L-M or S-Lum value for our CRT monitor. Hence, the chromatic contrasts of L-M and S-Lum are not perceptually equivalent. In separate sessions, stimuli were presented either in the affected (red in Figure S4) or normal (blue in Figure S4) hemifields.

Consideration of Previous Results

Our results provide positive quantitative evidence for some residual saliency computation even when V1 is absent, and hence when V1 cannot support the computation of the low-level visual features contributing to saliency. We found that motion was the strongest feature contributing to saliency-guided eye movements (Figure 3D) in normal monkeys, likely because we use dynamic stimuli where motion provides important clues to interesting objects. Motion remained strong in the affected hemifield of lesioned monkeys, consistent with laboratory experiments [28] and probably supported by geniculo-extrastriate and retino-tectal pathways [29-33]. That the unique contribution of orientation is nearly abolished in the affected field is not surprising given that our Gabor filters approximate canonical V1 simple cells [34]. Moreover, while blindsight patients can discriminate orientation of bars (e.g., horizontal vs. vertical), discrimination of the orientation of a grating in a circular aperture, which is a better test for sensitivity in orientation than using a single bar, was at chance level in patient GY, one of the well-studied blindsight patients [35]. This is consistent with our results that isolated the contribution of orientation. Note, however, that blindsight subjects can detect – in forced-choice paradigms – flickering oriented gratings, with relatively low spatial frequencies (e.g., [15]) as used in our model (less than 2 cycles/degree). Two differences may exist: first, ability to detect a feature when forced might not necessarily render that feature important in spontaneously guiding attention; second, our orientation saliency model is purely spatial, while stimuli used in previous experiments also had a temporal component (flickering, onset transients). The unique contribution of luminance was weak in normal monkeys but stronger in lesioned monkeys (Figure 3D). This is not contradictory to our previously reported decreased sensitivity to luminance [2]; indeed our results here simply show that despite decreased sensitivity, lesioned monkeys strategically relied more on luminance to decide where to look. Residual guidance to color stimuli was a more surprising prediction of our computational analysis [30, 31, 36-38]. The non-zero contribution of chromatic features in the affected field supports non-zero sensitivity for color in blindsight, for both L-M and S-cone chromatic features. Furthermore, our model predicts a stronger role for S-cone dependent signals in blindsight compared to control. This may reflect a strategic change in allocating attention given the impoverished residual feature representations postlesion or retrograde degeneration of retinal ganglion cells with selective loss of P beta cells depending on the time after the lesion [39-41]. It should be noted that the P beta cells, which are responsible for color-opponent processing, are not completely eliminated (e.g., 85% loss of P beta cells 8 years after lesions in [39]) and the small number of surviving cells may contribute to residual guidance to color saliency. Our control experiments confirm that monkeys with V1 lesion are sensitive not only to L-M but also to S-cone signals, and validate our computational prediction. It is interesting to note that the relatively poorer performance in L-M stimuli than in S-Lum stimuli (Figure S4A-B and S4C-D) may be explained by the reduced number of P beta cells by the retrograde degeneration [39-41]. Prior studies found no sensitivity to S-cone stimuli in human blindsight [30, 31] and no color sensitivity in the retino-tectal pathway of normal monkeys [42]. However, our results provide converging evidence with both free-viewing and laboratory stimuli for retained chromatic processing in

blindsight monkeys. That such residual chromatic processing may contribute to preattentive guidance of attention and gaze is not necessarily contradictory to previous findings that color discrimination or identification can be abolished in blindsight [43], as detection and discrimination may recruit distinct mechanisms. In a control task, we varied the luminance of chromatic targets and tested localization performance. Performance was higher than chance at all possible levels of luminance (Figure 4C), consistent with a previous report (localization task similar to ours but with reaching instead of saccades) where performance was higher than chance when stimuli were red or blue [37]. It is still an open question to determine the pathways for chromatic processing in blindsight, given possible global reorganization of pathways in the brain, as demonstrated in V1-lesioned animals [44] and patients [45].

In the free-viewing condition, subjects have no alerting cue for when to make saccades. Previous studies about human and monkey blindsight [46-48] suggest that cueing facilitates residual vision, in a way that may depend on the age of the lesion. However, we also note that cueing is not necessary for blindsight [49]. Our study shows that our blindsight monkeys spontaneously shifted their attention to natural, complex stimuli without alerting cues.

Supplemental References

1. Judge, S.J., Richmond, B.J., and Chu, F.C. (1980). Implantation of magnetic search coils for measurement of eye position: an improved method. *Vision Res* 20, 535-538.
2. Yoshida, M., Takaura, K., Kato, R., Ikeda, T., and Isa, T. (2008). Striate cortical lesions affect deliberate decision and control of saccade: implication for blindsight. *J Neurosci* 28, 10517-10530.
3. Champion, J., Latto, R., & Smith, Y. M. (1983). Is blindsight an effect of scattered light, spared cortex and near-threshold vision? *Behav Brain Sci* 3, 423-486.
4. Fendrich, R., Wessinger, C.M., and Gazzaniga, M.S. (1992). Residual vision in a scotoma: implications for blindsight. *Science* 258, 1489-1491.
5. Daniel, P.M., and Whitteridge, D. (1961). The representation of the visual field on the cerebral cortex in monkeys. *J Physiol* 159, 203-221.
6. Gattass, R., Gross, C.G., and Sandell, J.H. (1981). Visual topography of V2 in the macaque. *J Comp Neurol* 201, 519-539.
7. Van Essen, D.C., Drury, H.A., Dickson, J., Harwell, J., Hanlon, D., and Anderson, C.H. (2001). An integrated software suite for surface-based analyses of cerebral cortex. *J Am Med Inform Assoc* 8, 443-459.
8. Berg, D.J., Boehnke, S.E., Marino, R.A., Munoz, D.P., and Itti, L. (2009). Free viewing of dynamic stimuli by humans and monkeys. *J Vis* 9, 19 11-15.
9. Finney, S.A. (2001). Real-time data collection in Linux: a case study. *Behav Res Methods Instrum Comput* 33, 167-173.
10. Itti, L. (2005). Quantifying the contribution of low-level saliency to human eye movements in dynamic scenes. *Vis Cogn* 12, 1093-1123.
11. Robinson, D.A. (1963). A Method of Measuring Eye Movement Using a Scleral Search Coil in a Magnetic Field. *IEEE Trans Biomed Eng* 10, 137-145.
12. Itti, L. (2004). The iLab Neuromorphic Vision C++ Toolkit: Free tools for the next generation of vision algorithms. *The Neuromorphic Engineer* 1, 10.
13. Itti, L., and Koch, C. (2001). Computational modelling of visual attention. *Nat Rev Neurosci* 2, 194-203.
14. Itti, L., Koch, C., and Niebur, E. (1998). A model of saliency-based visual attention for rapid scene analysis. *IEEE T Pattern Anal* 20, 1254-1259.
15. Sahraie, A., Trevethan, C.T., Weiskrantz, L., Olson, J., MacLeod, M.J., Murray, A.D., Dijkhuizen, R.S., Counsell, C., and Coleman, R. (2003). Spatial channels of visual processing in cortical blindness. *Eur J Neurosci* 18, 1189-1196.
16. Parkhurst, D.J., and Niebur, E. (2003). Scene content selected by active vision. *Spat Vis* 16, 125-154.

17. Reinagel, P., and Zador, A.M. (1999). Natural scene statistics at the centre of gaze. *Network* 10, 341-350.
18. Tatler, B.W., Baddeley, R.J., and Gilchrist, I.D. (2005). Visual correlates of fixation selection: effects of scale and time. *Vision Res* 45, 643-659.
19. Baldi, P., and Itti, L. (2010). Of bits and wows: A Bayesian theory of surprise with applications to attention. *Neural Netw* 23, 649-666.
20. Itti, L., and Baldi, P. (2009). Bayesian surprise attracts human attention. *Vision Res* 49, 1295-1306.
21. Dantzig, G.B., and Thapa, M.N. (1997). *Linear programming 1: introduction*, (Secaucus, NJ, USA Springer-Verlag New York, Inc).
22. Itti, L. (2000). *Models of Bottom-Up and Top-Down Visual Attention*. Volume Ph.D. (California Institute of Technology), p. Chapter 7.10.
23. Krauskopf, J., Williams, D.R., and Heeley, D.W. (1982). Cardinal directions of color space. *Vision Res* 22, 1123-1131.
24. Derrington, A.M., Krauskopf, J., and Lennie, P. (1984). Chromatic mechanisms in lateral geniculate nucleus of macaque. *J Physiol* 357, 241-265.
25. Stockman, A., and Sharpe, L.T. (2000). The spectral sensitivities of the middle- and long-wavelength-sensitive cones derived from measurements in observers of known genotype. *Vision Res* 40, 1711-1737.
26. Baylor, D.A., Nunn, B.J., and Schnapf, J.L. (1987). Spectral sensitivity of cones of the monkey *Macaca fascicularis*. *J Physiol* 390, 145-160.
27. Dobkins, K.R., Thiele, A., and Albright, T.D. (2000). Comparison of red-green equiluminance points in humans and macaques: evidence for different L:M cone ratios between species. *J Opt Soc Am A Opt Image Sci Vis* 17, 545-556.
28. Weiskrantz, L., Barbur, J.L., and Sahraie, A. (1995). Parameters affecting conscious versus unconscious visual discrimination with damage to the visual cortex (V1). *Proc Natl Acad Sci U S A* 92, 6122-6126.
29. Mohler, C.W., and Wurtz, R.H. (1977). Role of striate cortex and superior colliculus in visual guidance of saccadic eye movements in monkeys. *J Neurophysiol* 40, 74-94.
30. Leh, S.E., Mullen, K.T., and Ptito, A. (2006). Absence of S-cone input in human blindsight following hemispherectomy. *Eur J Neurosci* 24, 2954-2960.
31. Tamietto, M., Cauda, F., Corazzini, L.L., Savazzi, S., Marzi, C.A., Goebel, R., Weiskrantz, L., and de Gelder, B. (2010). Collicular vision guides nonconscious behavior. *J Cogn Neurosci* 22, 888-902.
32. Sincich, L.C., Park, K.F., Wohlgenuth, M.J., and Horton, J.C. (2004). Bypassing V1: a direct geniculate input to area MT. *Nature Neurosci* 7, 1123-1128.
33. Schmid, M.C., Mrowka, S.W., Turchi, J., Saunders, R.C., Wilke, M., Peters, A.J., Ye, F.Q., and Leopold, D.A. (2010). Blindsight depends on the lateral geniculate nucleus. *Nature* 466, 373-377.
34. Daugman, J.G. (1980). Two-dimensional spectral analysis of cortical receptive field profiles. *Vision Res* 20, 847-856.
35. Morland, A.B., Ogilvie, J.A., Ruddock, K.H., and Wright, J.R. (1996). Orientation discrimination is impaired in the absence of the striate cortical contribution to human vision. *Proc Biol Sci* 263, 633-640.
36. Marzi, C.A., Mancini, F., Metitieri, T., and Savazzi, S. (2009). Blindsight following visual cortex deafferentation disappears with purple and red stimuli: a case study. *Neuropsychologia* 47, 1382-1385.
37. Cowey, A., and Stoerig, P. (2001). Detection and discrimination of chromatic targets in hemianopic macaque monkeys and humans. *Eur J Neurosci* 14, 1320-1330.
38. Brent, P.J., Kennard, C., and Ruddock, K.H. (1994). Residual colour vision in a human hemianope: spectral responses and colour discrimination. *Proc Biol Sci* 256, 219-225.

39. Cowey, A., Alexander, I., and Stoerig, P. (2011). Transneuronal retrograde degeneration of retinal ganglion cells and optic tract in hemianopic monkeys and humans. *Brain* 134, 2149-2157.
40. Cowey, A., Stoerig, P., and Perry, V.H. (1989). Transneuronal retrograde degeneration of retinal ganglion cells after damage to striate cortex in macaque monkeys: selective loss of P beta cells. *Neuroscience* 29, 65-80.
41. Weller, R.E., Kaas, J.H., and Wetzel, A.B. (1979). Evidence for the loss of X-cells of the retina after long-term ablation of visual cortex in monkeys. *Brain Res* 160, 134-138.
42. White, B.J., Boehnke, S.E., Marino, R.A., Itti, L., and Munoz, D.P. (2009). Color-related signals in the primate superior colliculus. *J Neurosci* 29, 12159-12166.
43. Alexander, I., and Cowey, A. (2010). Edges, colour and awareness in blindsight. *Conscious Cogn* 19, 520-533.
44. Payne, B.R., and Lomber, S.G. (2001). Reconstructing functional systems after lesions of cerebral cortex. *Nat Rev Neurosci* 2, 911-919.
45. Bridge, H., Thomas, O., Jbabdi, S., and Cowey, A. (2008). Changes in connectivity after visual cortical brain damage underlie altered visual function. *Brain* 131, 1433-1444.
46. Moore, T., Rodman, H.R., Repp, A.B., Gross, C.G., and Mezrich, R.S. (1996). Greater residual vision in monkeys after striate cortex damage in infancy. *J Neurophysiol* 76, 3928-3933.
47. Moore, T., Rodman, H.R., Repp, A.B., and Gross, C.G. (1995). Localization of visual stimuli after striate cortex damage in monkeys: parallels with human blindsight. *Proc Natl Acad Sci U S A* 92, 8215-8218.
48. Kentridge, R.W., Heywood, C.A., and Weiskrantz, L. (1999). Effects of temporal cueing on residual visual discrimination in blindsight. *Neuropsychologia* 37, 479-483.
49. Stoerig, P. (2010). Cueless blindsight. *Front Hum Neurosci* 3, 74.